The Eurasia Proceedings of Science, Technology, Engineering & Mathematics (EPSTEM)
ISSN: 2602-3199

The Eurasia Proceedings of Science, Technology, Engineering & Mathematics (EPSTEM), 2022

Volume 21, Pages 116-124

IConTES 2022: International Conference on Technology, Engineering and Science

Effect of Protan Recoloring Algorithm on Inserted Watermark in Presence of the Superimposed AWGN

Zoran MILIVOJEVIC
Academy of Applied Technical and Preschool Studies

Bojan PRLINCEVIC
Kosovo and Metohija Academy Division Zvecan

Abstract: In this paper, the effect of the protan recoloring algorithm on an image with an inserted watermark is analyzed. In addition, the effect of degradation of the quality of the recolored image due to the insertion of watermarks and superimposed AWGN was also analyzed. In the first part of the paper, the effect of color vision deficiency, as a consequence of anomalies in L cones, which is designated as protanomaly (protanopia), is described. People with protanopia do not see a wide range of colors because the colors from the L channel are missing. After that, the recoloring algorithm, which performs recoloring of the image, so that, in protan persons, the visible spectrum of colors is expanded, is described. Then, the algorithm for inserting a watermark, in order to protect copyrights, is described. In the second part of the work, the Experiment, in which the quality of the recoloring image was tested, as well as the quality of the extracted watermark, was described. The results of the experiment are shown with pictures and tables. By applying a comparative analysis of the results of the experiment, using objective (MSE, PSNR, NC and SSIM) and subjective (visual inspection) methods, the insertion factor of the watermark, α, which preserves the quality of the recoloring image as well as the quality of the extracted watermark, was determined. Visual inspection determined the SNR at which visible image degradation and watermarks occur.

Keywords: Trichromacy, Protanomaly, Image recoloring, Watermark, SVD algorithm

Introduction

Many algorithms in digital image processing are conceptually designed in accordance with the Human Visual System (HVS). The first organ in the HSV is the eye. Therefore, for quality digital image processing, it is necessary to have a good understanding structure of the human eye. It is very important to understand the distribution and functions of photoreceptors on the retina. The photoreceptors are a special type of neurons, which are sensitive to the effect of the light. The wavelength range of the light, that HSV can detect, is λ = 370 - 720 nm (Curcio et al., 1990). According to the spectral characteristics, the photoreceptors can be divided into two groups: a) sensitive to light intensity (luminance) and b) sensitive to the quality, that is, the color of the light. The photoreceptors that are sensitive to the intensity of the light, according to their physical appearance, are in the form of rods. The human eye has about 120,000,000 rods. Functionally, their role is to enable so-called black-white vision. They are extremely sensitive to light intensity and enable vision even at very low intensities (night vision). The photoreceptors that are sensitive to the color of the light have the physical shape of cones. The human eye has about 6,000,000 cones. The cones are mostly concentrated in the central parts of the retina. The cones are sensitive to the color of light, especially at higher brightness levels. From the point of view of spectral sensitivity, there are three types of the cone. The first type are the cones that are sensitive to light in the long wavelength range, $L(\lambda)$. In the L range, the red color, R, is dominant. Another type of the cones are sensitive to light in the medium wavelength range, $M(\lambda)$. In the M range, the dominant color is green, G. The third type of the cones are sensitive to light in the range of short wavelengths, $S(\lambda)$. In people who do not have

- This is an Open Access article distributed under the terms of the Creative Commons Attribution-Noncommercial 4.0 Unported License, permitting all non-commercial use, distribution, and reproduction in any medium, provided the original work is properly cited.

- Selection and peer-review under responsibility of the Organizing Committee of the Conference

© 2022 Published by ISRES Publishing: www.isres.org

functional vision problems, rods and all three types of cones function properly. Such people have so-called normal or trichromatic vision (Blake & Sekuler, 2006).

Color is created in the consciousness of the observer, as the brain processes signals from L, M and S cones (Zhenyang et al., 2021). Statistically speaking, over 200,000,000 people around the world have problems with color perception. Color vision deficiency, CVD, occurs when one, two or all types of the cones do not function correctly. CVD can be classified as anomalous type: a) trichromacy (some types of the cones do not function in their visual range, but are shifted to one frequency side), b) dichromacy (with this anomaly there are only two types of the cones, which are capable of perceiving color. The functions of the third type of the cones are completely inactive); and c) monochromacy (none of the cones are active. Only the rods are active and enable black-and-white vision) (Milivojevic et al., 2022). In order to help CVD people see a wider range of the colors in the observed image, it is necessary to perform image pre-processing to correct the types of colors in the image (Nam et al., 2005). This process is, in the scientific literature, called Recoloring (Zhenyang et al., 2021), (Lin et al., 2019).

Intensive exchange of the images over the Internet enables unauthorized use of the images. For this reason, there was a need to protect the Recoloring (RC) image from unauthorized use. One of the ways of copyright protection is to insert watermarks into the image. The watermark can be: a) visible and b) invisible. The visible watermark clearly indicates the owner of the image. However, the visible watermark degrades the image quality. The invisible watermark is inserted into the RC image in the transformation domain, and does not perform visible degradation. On the other hand, it is possible to extract it from the RC image, and, in this way, prove the ownership of the image. The paper (Pramoun et al., 2017) describes an algorithm for inserting and extracting watermarks from RC images, which was created for protan CVD people. Protan CVD is an anomaly of the *L* cones such that their spectral sensitivity is sifted in the direction of the spectral sensitivity of the *M* cones. In order to insert the watermarks, using the Block SVD (Singular Value Decomposition) algorithm, the RC image processing is realized in the LMS color space (Pramoun et al., 2018) (Crenshaw, 2014).

In this paper, the effect of the protan RC algorithm on the inserted watermark is analyzed. First, the RC algorithm (Crenshaw, 2014) is described. After that, the modified Block SVD watermarking (Chang et al., 2007) is described. The modification was made by the authors of this paper. The second part of the paper describes an Experiment in which the performance of the Blok SVD watermark was tested on: a) protan RC algorithm, and b) superimposed AWGN. Additionally, the effect of inserted watermark and superimposed AWGN on quality of the RC image was analyzed. The algorithm, according to which the Experiment was carried out, is presented. The Test image, on which recoloring was performed, is *Flowers*. The inserted Watermark was the *Logo* of Academy of Applied Technical and Preschool Studies, Niš, Serbia. The performance of extracted watermark and RC image was tested using: a) objective measures (MSE, PSNR, NC and SSIM), and b) visual inspection. The results of the Experiment are RC image and extracted watermarks. In addition, the numerical results for are shown using graphs. Based on the results, a comparative analysis was performed and conclusions were drawn about the effects of the RC algorithm and AWGN on watermark performance.

Further organization of work is as follows. In Section II, CVD anomalous is presented. In Section III, the Recoloring algorithm for protanopia, is presented. In Section IV, the Watermarking algorithm, is described. In Section V the Experiment, is described. Section VI is the Conclusion.

CVD Anomalous

In people with normal (trichromatic) vision, color images are perceived using all of three types of cones (LMS). In people with color vision deficiency (CVD), some or even all types of cones do not function correctly. According to the type of cones that do not function correctly, CVD is classified as: a) trichromacy, b) dichromacy, or c) monochromacy. CVD trichromacy is an anomaly when one type of the cones does not function correctly. An anomaly in the CVD dichromacy is that one of the tip cones does not work. With CVD monochromacy anomaly, neither type of cones works. Therefore, people with CVD monochromacy see only with rods photoreceptors, that is, they have monochromatic vision (lumination, black-and-white vision). CVD trichromacy and dichromacy, depending on whether the abnormalities occur in *L*, *M* or *S* cones, can be classified as: a) protan, (abnormalities occur in *L* cones), b) deutan (abnormalities occur in *M* cones) or c) tritan (abnormalities occur in *S* cones) defects. Protan, deutan and tritan defects in anomalous trichromacy and dichromacy are called protanomaly (protanopia), deuteranomaly (deuteranopia) or tritanomaly (tritanopia), respectively (Milivojevic et al., 2022).

In fig. 1.a shows the normalized spectral sensitivity of human cone cells of: a) short $S(\lambda)$, b) middle $M(\lambda)$ and c) long $L(\lambda)$ wavelength types. The cones, which have these spectral characteristics of sensitivity, enable normal, that is, trichromatic vision. In the consciousness of the observer, the feeling of the presence of colors from the entire visible spectrum (fig. 1.b) is formed. Protanomaly is an abnormal trichromacy, which is a consequence of the poor functionality of the L cones (Zhenyang et al., 2021). In this case, the spectral sensitivity of the L cones is shifted by $\Delta\lambda$ in the direction of the spectral sensitivity of the M cones. In protan CVD, the spectral sensitivity is $L_a(\lambda) = L_a(\lambda + \Delta\lambda)$, where $\Delta\lambda$ = (0 - 20) nm, that is, protan is 0 - 100%. In fig. 1.c shows the spectral sensitivities of the L cones for 100% protan CVD. The color experience of 100% protan CVD people is shown in fig. 1. d.

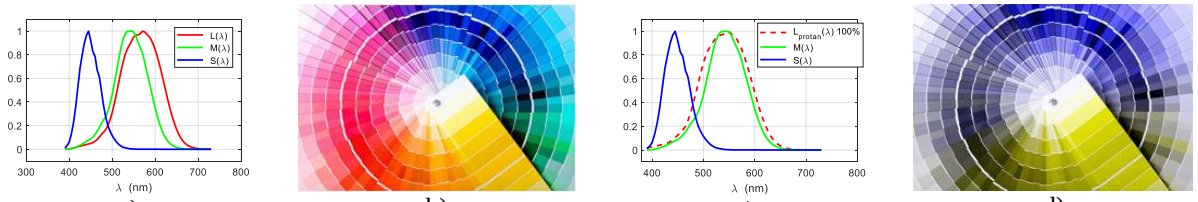

a) b) c) d)

Figure 1. a) Normalized spectral sensitivity of human cone cells of short $S(\lambda)$, middle $M(\lambda)$ and long $L(\lambda)$ wavelength types with normal vision. b) test image Spectrum, c) spectral sensitivity of the L cones at 100% protan CVD, and d) color experience of 100% protan CVD people.

CVD protan people often cannot see all the color details in the image. In order to reduce this discomfort, it is possible to perform color correction (recoloring) in the image so that people with CVD protan problem can see better. Image recoloring is the creation of a different version of the image colors that is more suitable for such people.

Recoloring Algorithm for Protan CVD

In (Crenshaw, 2014) the Recoloring (RC) algorithm for the protanopia CVD class, is described. The RC algorithm is implemented using color transformation in the LMS color space. The RC algorithm is implemented in the following steps:

Input: I - Original image in the RGB color space.
Output: I_{RC} - Recolored image in the RGB color space

Step 1: Image transformation from RGB color space (I_{RGB}) to the LMS color space (I_{LMS}):

$$\begin{bmatrix} L \\ M \\ S \end{bmatrix} = \begin{bmatrix} 17.8824 & 43.5161 & 4.11935 \\ 3.45565 & 27.1554 & 3.86714 \\ 0.0299566 & 0.184309 & 1.46709 \end{bmatrix} \times \begin{bmatrix} R \\ G \\ B \end{bmatrix}, \quad (1)$$

where R, G and B are red, green and blue color components of image I in RGB color space.

Step 2: Simulated color perception of CVD protan people:

$$\begin{bmatrix} L_p \\ M_p \\ S_p \end{bmatrix} = \begin{bmatrix} 0 & 2.02344 & -2.52581 \\ 0 & 1 & 0 \\ 0 & 0 & 1 \end{bmatrix} \times \begin{bmatrix} L \\ M \\ S \end{bmatrix}. \quad (2)$$

where L_p, M_p and S_p are the simulated components in the LMS state space.

Step 3: Error between normal and color-blind perception in LMS color space:

$$\begin{bmatrix} E_L \\ E_M \\ E_S \end{bmatrix} = \begin{bmatrix} L \\ M \\ S \end{bmatrix} - \begin{bmatrix} L_p \\ M_p \\ S_p \end{bmatrix}. \quad (3)$$

Step 4: The errors are redistributed to the other two visible color components, i.e. M and S color components by applying the below transformation.

$$\begin{bmatrix} E_{L\_MOD} \\ E_{M\_MOD} \\ E_{S\_MOD} \end{bmatrix} = \phi \begin{bmatrix} -0.2 & 0 & 0 \\ 0.1 & 1 & 0 \\ 0.1 & 0 & 1 \end{bmatrix} \times \begin{bmatrix} E_L \\ E_M \\ E_S \end{bmatrix}, \quad (4)$$

where E_{L_MOD}, E_{M_MOD}, and E_{S_MOD}, are the portion of error from colors associated with color blind to colors associated with normal perception (Chang et al., 2007), and ϕ is a scalar value between 0 to 1, and is used to vary the chrominance strength.

Step 5: The recolored image (RC image) in the LMS color space is:

$$\begin{bmatrix} L_{p,RE} \\ M_{p,RE} \\ S_{p,RE} \end{bmatrix} = \begin{bmatrix} E_{L\_MOD} \\ E_{M\_MOD} \\ E_{S\_MOD} \end{bmatrix} + \begin{bmatrix} L \\ M \\ S \end{bmatrix}. \quad (5)$$

Step 7: The RC image in the RGB color space is:

$$\begin{bmatrix} R_{re} \\ G_{re} \\ B_{re} \end{bmatrix} = \begin{bmatrix} 0.080944 & -0.130504 & 0.11672 \\ -0.01025 & 0.054019 & -0.11362 \\ -0.00037 & -0.004122 & 0.69351 \end{bmatrix} + \begin{bmatrix} L_{p,RE} \\ M_{p,RE} \\ S_{p,RE} \end{bmatrix} \quad ,(6)$$

where R_{re}, G_{re}, and B_{re} are the colored components in the RGB color space (RC image, I_{RC}).

An example of processing the Test image, which is presented in the RGB color space, using the RC algorithm. The Test image is shown in fig. 2.a. Protan CVD person perceives colors as in fig. 2.b. (BL image, *Step 2*). After color correction, the protan CVD person experiences colors as in fig. 2.c (RC image, *Step 7*). From the described example, it can be concluded that the effect of the image processing using the RC algorithm led to an increased range of color perception.

a) b) c)

Figure 2. a) Test image, b) BL image and c) RC image.

Block SVD Watermarking Algorithm

The Block SVD Watermarking Algorithm is presented in (Chang et al., 2007). It is based on the embedded of one bit of the watermark in one 4 x 4 image block. In this paper, embedding of the watermark is done in a color image. Embedding of the watermark is done in the *M* component of the image in the LMS color space.

Watermark Embedding Algorithm

Input: *I* - image in the RGB color space. *W* - watermark (Mw_m x Nw_m). Insertion factor α.
Output: *Iw* - watermarked image

Step 1: Transformation of image *I* from RGB color space (I_{RGB}) to LMS color space (I_{LMS}).
Step 2: Extracting the *M* component from the image I_{LMS}.
Step 3: The image component *M* is divided into non-overlapping blocks *B* dimension 4 x 4.
FOR $i = 1 : Mw_m$
FOR $j = 1 : Nw_m$
Step 4: Selecting (*i, j*) block, $B_{i,j}$, of the *M* image component.
Step 5: SVD transformation of the block $B_{i,j}$:

$$B_{i,j} = U_{i,j} \times S_{i,j} \times V_{i,j}^T, \quad (7)$$

where $U_{i,j}$ and $V_{i,j}$ are orthogonal matrices, $U_{i,j} = [u_1\ u_2\ u_3\ u_4]$ and , $V_{i,j} = [v_1\ v_2\ v_3\ v_4]^T$, respectively, while $S_{i,j}$ is a diagonal matrix $S_{i,j} = \text{diag}(\sigma_1, \sigma_2, \sigma_3, \sigma_4)$.
Step 6: Assigning the value $\sigma_{3n} = \sigma_2$.
Step 7: Inserting the bit $W_{i,j}$ of the watermark *W*: $\sigma_{2n} = \sigma_2 + \alpha \cdot W_{i,j}$.
Step 8: Modification of the matrix *S* according to: **IF** $\sigma_1 < \sigma_{2n}$ **THEN** $\sigma_{1n} = \sigma_{2n}$; **ELSE** $\sigma_{1n} = \sigma_1$; **END**, after which the diagonal matrix with watermark bit is matrix $Sw_{i,j} = \text{diag}(\sigma_{1n}, \sigma_{2n}, \sigma_{3n}, \sigma_4)$.
Step 9: Reconstruction of the block with the mark $Bw_{i,j}$:
Step 10: Reconstructing the *Mw* component with the embed watermark $Mw \Leftarrow Bw_{i,j}$.
END *j*
END *i*
Step 11: The reconstructed image with the watermark (Iw_{LMS}) is translated from the LMS color space into the RGB color space (Iw_{RGB}), and the image with the embedded watermark *Iw* is finally obtained.

Watermark Extraction Algorithm

Input: *Iw* - Image with watermark. Mw_m x Nw_m - dimensions of watermark block. α - insertion factor.
Output: *We* - extracted watermark.
Step 1: Transformation of image *Iw* from RGB color space (Iw_{RGB}) to LMS color space (Iw_{LMS}).
Step 2: Extracting the *Mw* component from the image Iw_{LMS}.
Step 3: The image component *Mw* is divided into non-overlapping blocks *Bw*, dimension 4 x 4.
FOR $i = 1 : Mw_m$
FOR $j = 1 : Nw_m$
Step 4: Selecting (*i, j*) block, $Bw_{i,j}$, of the *Mw* image component.
Step 5: SVD transformation of the block $Bw_{i,j}$:

$$Bw_{i,j} = U_{i,j} \times Sw_{i,j} \times V_{i,j}^{T} . \quad (8)$$

Step 6: The values of the watermark bit, $We_{i,j}$, which is extracted from the block $Bw_{i,j}$ are determined according to **IF** $\sigma_2 < \sigma_3$; **THEN** $We_{i,j} = 1$; **ELSE** $We_{i,j} = 0$; **END**.
END *j*
END *i*

Experimental Results and Result Analysis

Experiment

An Experiment, in which the tested robustness of the Blok SVD watermark to: a) recoloring of the image for protan CVD people, and b) superimposed AWGN with some SNR values, was realized. The RC algorithm for the protanopia CVD class is used for recoloring of the Test image. After inserting the watermark into the Test image, AWGN, with SNR = {0, 10, 20, 30, 40, 50} dB, is superimposed. The performance of the extracted watermark, as well as the RC image, was tested using: a) objective measures, and b) visual inspection. Standard objective measures, which are intensively used in digital signal processing, especially in digital image processing: a) Mean Square Error, MSE, b) Peak Signal to Noise Ratio, PSNR, c) Normalized Correlation, NC and d) Structure Similarity Index, SSIM, were used. The Experiment was done in the following steps:

Input: *I* - Test image in the RGB color space. *W* - binary watermark. Insertion factor α.
Output: Objective measures MSE, PSNR, NC and SSIM.
Step 1: Inserting a watermark *W* into Test image *I* with the insertion factor α, and creating an image with a watermark I_{WM}.
Step 2: Superimpose AWGN to Test image with inserted watermak I_{WM}. and create image $I_{WM,AW}$ with specified SNR.
Step 3: Changing the colors of the image $I_{WM,AW}$ by applying the RC algorithm, RC image with changed colors, which are adapted to Protain CVD persons, are created.
Step 4: Extracting watermark *We* from RC image.
Step 5: Visual inspection of the RC image and determination of α_C at which the watermark begins to be seen in the image.
Step 6: Visual inspection of the RC image and determination of the SNR_C at which the AWGN begins to be seen in the image.
Step 7: Determining the performance of the extracted watermark *We* and RC image using MSE, PSNR, NC and SSIM measures.

The results of the objective measure are shown graphically. After that, a comparative analysis of the results is presented.

Base

For the Experiment purposes the Image database was created. The Image database is made up of: a) Test image *Flowers*, 200 x 256 pixels, (fig. 3.a), and b) an electronic watermark (*Logo* of Academy of Applied Technical and Preschool Studies, Niš, Serbia), 32 x 32 pixels. In order to distribute the watermark over the entire Test image, a new watermark (50 x 64 pixels), which was obtained from multiple repetitions of the Logo (fig. 4.a), was created.

Results

The Test image used in this experiment is shown in fig. 3.a. By applying the RC algorithm, the following were obtained: a) Color blind image (CB image), which is with colors as they are perceived by protan CVD people (fig. 3.b), and b) Recolored image (RC image) whose colors are perceived by CVD protons as a wide spectrum

(fig. 3.c). The binary watermark, which was created by spatial repetition of the Logo of Academy of Applied Technical and Preschool Studies, is shown in fig. 4. a. The RC image with inserted watermark is shown in fig. 6, for the values of the insertion factor: a) $\alpha = 0$, b) $\alpha = 0.02$, c) $\alpha = 0.05$, d) $\alpha = 0.1$, and e) $\alpha = 0.3$. RC image with superimposed AWGN, for $\alpha = 0$, is shown in fig. 7: a) SNR = 50 dB, b) SNR = 20 dB, c) SNR = 10 dB, d) SNR = 0 dB, e) SNR = -10 dB. By applying the Blok SVD watermarking algorithm, the binary watermark was inserted and extracted for the insertion factor $\alpha = 0 - 0.3$, with a step of $\Delta\alpha = 0.001$. The extracted watermarks, for SNR = 50 dB, are shown in fig. 4.b ($\alpha = 0.02$), fig. 4.c ($\alpha = 0.05$), fig. 4.d ($\alpha = 0.1$) and fig. 4.e ($\alpha = 0.3$). The extracted watermarks, for insertion factor $\alpha = 0.02$, are shown in fig. 5.b (SNR = 50 dB), fig. 5.c (SNR = 40 dB), fig. 5.d (SNR = 30 dB), and fig. 5.e (SNR = 20 dB). RC images are shown in: fig. 6.a ($\alpha = 0$), fig. 6.b ($\alpha = 0.02$), fig.6.c ($\alpha = 0.05$), fig. 6.d ($\alpha = 0.1$) and fig. 6.e ($\alpha = 0.3$). The objective measurements, determined between the original and extracted watermarks, depending on the SNR, are shown in: a) fig. 8.a (MSE), b) fig. 8.b (PSNR), c) fig. 8.c (NC), and d) fig. 8.d (SSIM). The objective measurements, determined between the Test image and Test image with inserted watermark, depending on the SNR, are shown in a) fig. 9.a (MSE), b) fig. 9.b (PSNR), c) fig. 9.c (NC) and d) fig. 9.d (SSIM). The objective measurements, determined between the RC image and RC image with inserted watermark, depending on the SNR, are shown in a) fig. 10.a (MSE), b) fig. 10.b (PSNR), c) fig. 10.c (NC) and d) fig. 10.d (SSIM).

a) b) c)

Figure 3. a) Test image *Flowers*, b) CB image and c) RC image.

a) b) c) d) e)

Figure 4. a) Watermark (*Logo*). Extracted Watermark, for SNR = 50 dB, for insertion factor: b) $\alpha = 0.02$, c) $\alpha = 0.05$, d) $\alpha = 0.1$, e) $\alpha = 0.3$

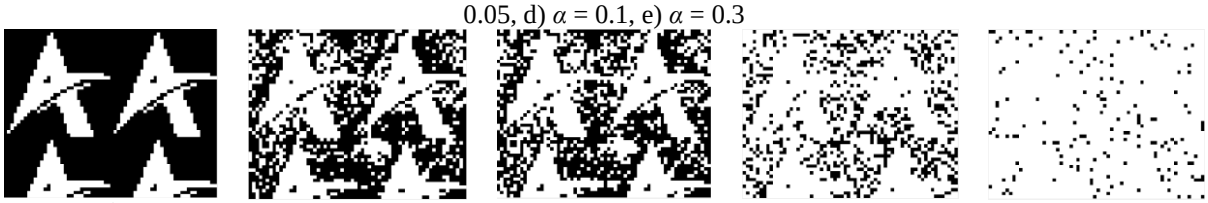

a) b) c) d) e)

Figure 5. a) Watermark (*Logo*). The extracted watermarks, for insertion factor $\alpha = 0.02$: b) SNR = 50 dB c) SNR = 40 dB, d) SNR = 30 dB, e) SNR = 20 dB.

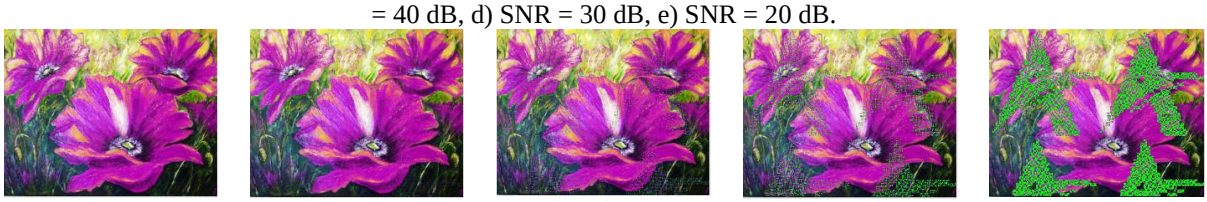

a) b) c) d) e)

Figure 6. The RC image with inserted watermark: a) $\alpha = 0$, b) $\alpha = 0.02$, c) $\alpha = 0.05$, d) $\alpha = 0.1$, e) $\alpha = 0.3$.

a) b) c) d) e)

Figure 7. RC slika sa superponiranim AWGN ($\alpha = 0$): a) SNR = 50 dB, b) SNR = 20 dB, c) SNR = 10 dB, d) SNR = 0 dB, e) SNR = -10 dB.

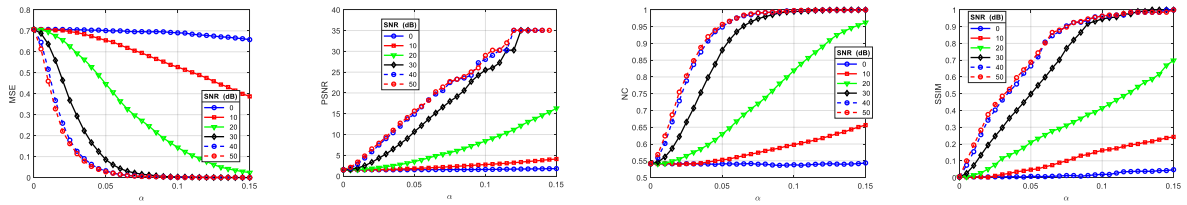

a) b) c) d)

Figure 8. The objective measurements between the original and extracted watermarks: a) MSE, b) PSNR, c) NC, and d) SSIM.

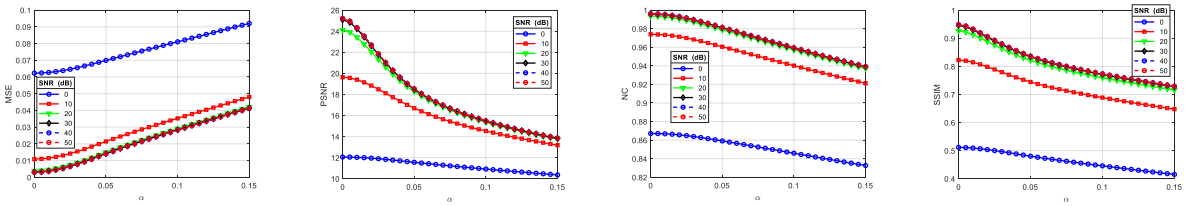

a) b) c) d)

Figure 9. Objective measurements between the Test image and Test image with inserted watermark, depending on the SNR,: a) MSE, b) PSNR, c) NC, and d) SSIM.

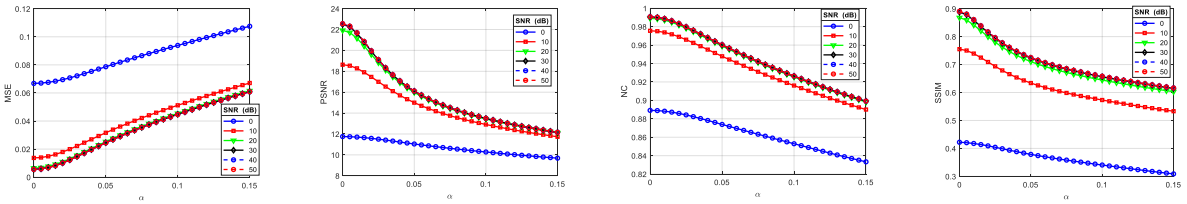

a) b) c) d)

Figure 10. Objective measurements between the RC image and RC image with inserted watermark, depending on the SNR, a) MSE, b) PSNR, c) NC, and d) SSIM.

Analysis of Results

Using the subjective method, which was realized by visual inspection of the quality of the RC image and extracted watermark, the critical value of the insertion factor $\alpha_C = 0.02$ (fig. 6.b), was determined. Increasing the insertion factor causes visible degradations in the RC image (fig. 6.c - fig. 6.e). The degradation of the RC image is such that the watermark becomes visible (fig. 6.e). However, increasing the insertion factor α causes an increase in the quality of the extracted watermark (fig. 4). The visual quality of the extracted watermark, which is inserted with the insertion factor α_C, is satisfactory, and as such it can be used to prove the ownership of the RC image (fig. 4.b). The visibility of the superimposed AWGN in the RC image was tested by visual inspection. Visibility of AWGN is beginning to occur at SNR_C. = 20 dB (fig. 7.d). RC image degradations increase with decreasing SNR (fig. 7.e). Visible degradations of the AWGN are distributed over the entire surface of the RC image. The effect of AWGN on the quality of the watermark, when the SNR is less than the SNR_C, is so degrading that the existence of the watermark in the RC image cannot be proven (fig. 5).

The objective measurements between the original and extracted watermarks, observing the graphics in fig. 8, for $\alpha_C = 0.02$, and SNR = 20 dB are: a) $MSE_{WM} = 0.6572$ (fig. 8.a), b) $PSNR_{WM} = 1.8231$ (fig. 8.b), c) $NC_{WM} = 0.5546$ (fig. 8.c) and d) $SSIM_{WM} = 0.0556$ (fig. 8.d). The objective measures of degradation of the Test image

with an inserted watermark and superimposed AWGN (fig. 7.a) compared to the Test image without a watermark and AWGN (fig. 3.a) are: a) MSE_{TI} = 0.0062 (fig. 9.a), b) $PSNR_{TI}$ = 22.0581 (fig. 9.b), c) NC_{TI} = 0.9904 (fig. 9.c) and d) $SSIM_{TI}$ = 0.8891 (fig. 9.d). The objective measures of degradation of the RC image with an inserted watermark and superimposed AWGN (fig. 7.a) compared to the RC image without a watermark and AWGN (fig. 3.c) are: a) MSE_{RC} = 0.0109 (fig. 10.a), b) $PSNR_{RC}$ = 19.6079 (fig. 10.b), c) NC_{RC} = 0.9817 (fig. 10.c), and d) $SSIM_{RC}$ = 0.8000 (fig. 10.d). An example of drastic degradation of the RC image (α = 0.3, SNR = 50 dB) is shown in fig. 6. e. The extracted watermark has excellent visual quality (fig. 4.e). Appropriate objective measures for watermarks are: a) MSE_{WM} = 0.00 (fig. 8.a), b) $PSNR_{WM} = \infty$ (fig. 8.b), c) NC_{WM} = 1.00 (fig. 8.c) and d) $SSIM_{WM}$ = 1.00 (fig. 8.d). Objective measures of the RC image are: a) MSE_{RC} = 0.0915 (fig. 10.a), b) $PSNR_{RC}$ = 10.3845 (fig. 10.b), c) NC_{RC} = 0.8555 (fig. 10.c) and d) $SSIM_{RC}$ = 0.5554 (fig. 10.d).

Objective measures, as well as subjective measures, indicate that increasing the insertion factor α affects the increase in the visual quality of the extracted watermark, as well as the decrease in the quality of the RC image. Also, objective measures, as well as subjective measures, indicate a significant degradation of the RC image due to the superimposed AWGN. The AWGN effect is particularly reflected in the quality of the extracted watermark. In order to increase the quality of the extracted watermark, the RC image should be pre-processed before extracting the watermark, which will be the following activities.

Conclusion

This paper describes an algorithm for recoloring images, which are intended for the protan CVD persons. For copyright purposes, a watermark has been inserted into the image using the Block SVD algorithm. In order to determine the quality of the watermark due to the effect of the RC algorithm, as well as the degradation of the RC image due to the effect of the watermark, an experiment was carried out. Additionally, AWGN superimposition was performed for some SNRs. The experimental results were analyzed using: a) subjective method (visual inspection), and b) objective measures (MSE, PSNR, NC and SSIM). Using a visual inspection, it was shown that, for the watermark insertion factor α_C = 0.02, there is an invisibility of the watermark in the image. In addition, it has been shown that the extracted watermark is of satisfactory quality for proving copyright. Visibility of AWGN is beginning to occur at SNR_C = 20 dB. Visible degradations of the AWGN are distributed over the entire surface of the RC image. Further reduction of the SNR leads to visible degradation of the RC image and extracted watermark.

Scientific Ethics Declaration

The authors declare that the scientific ethical and legal responsibility of this article published in EPSTEM journal belongs to the authors.

Acknowledgements or Notes

* This article was presented as an oral presentation at the International Conference on Technology, Engineering and Science (www.icontes.net) held in Antalya/Turkey on November 16-19, 2022.

References

Blake, R., & Sekuler, R. (2006). *Perception*. McGraw-Hill.

Chang, C., Hu, Y., & Lin, C. (2007). A digital watermarking scheme based on singular value decomposition. from *ESCAPE 2007 First International Symposium*, Hangzhou, 82–93.

Crenshaw, C. (2014). *Realtime color vision deficiency correction*, U.S. Patent: 20140066196 A1.

Curcio, C. A., Sloan, K. R., Kalina, R. E., & Hendrickson, A. E. (1990). Human photoreceptor topography. *J. Compar. Neurol*., *292*(4). 497–523.

Lin, H., Chen, L., &, Wang, M. (2019). Improving discrimination in color vision deficiency by image re-coloring. *Sensors*, *19*(10), 2250: 1-19.

Milivojevic, Z., Prlincevic, B., Kostic, D. (2022). Degradation recoloring cvd protan image from blok svd watermark, proceedings from erk 2022. *31th International Electrotechnical and Computer Science Conference*, Portoroz, Slovenia.

Nam, J., Yong, R., Huh, Y., &, Kim, M. (2005). Visual content adaptation according to user perception characteristics. *IEEE Transactions on Multimedia, 7*(3), 435–445.

Pramoun, T., Supasirisun, P., & Amornraksa, T. (2018). Digital watermarking on recolored images for protanopia. proceedings from *15th International Conference on Electrical Engineering/Electronics, Computer, Telecommunications and Information Technology*. 62 - 65.

Pramoun, T., Thongkor, K., & Amornraksa, T. (2017). Image watermarking against color blind image correction. proceedings from ubi-media. *10th International Conference on Ubi-media Computing and Workshops*, 1-6.

Zhenyang, Z., Toyoura, M., Go, K., Kashiwagi, K., Fujishiro, I., Wong, T., & Mao, X. (2021). Personalized image recoloring for color vision deficiency compensation. *IEEE Transactions on Multimedia*, 24, 1721 - 1734.

Author Information

Zoran Milivojevic
Academy of Applied Technical and Preschool Studies
A. Medvedeva 20, Nis, Serbia
e-mail: *zoran.milivojevic@akademijanis.edu.rs*

Bojan Prlincevic
Kosovo and Metohija Academy Division,
Zvecan, Serbia

To cite this article:

Milivojevic, Z. & Prlincevic, B. (2022). Effect of protan recoloring algorithm on inserted watermark in presence of the superimposed AWGN. *The Eurasia Proceedings of Science, Technology, Engineering & Mathematics (EPSTEM), 21*, 116-124.